ChemPubSoc Europe

DOI: 10.1002/chem.201801440

CHEMISTRY A European Journal Communication

Proteins

Soft X-ray Spectroscopy as a Probe for Gas-Phase Protein Structure: Electron Impact Ionization from Within

Sadia Bari,[a] Dmitrii Egorov,[b] Thomas L. C. Jansen,[b] Rebecca Boll,[a] Ronnie Hoekstra,[b] Simone Techert,[a, g] Vicente Zamudio-Bayer,[c, f] Christine Bülow,[c, d] Rebecka Lindblad,[c, e] Georg Leistner,[c, d] Arkadiusz Ławicki,[c] Konstantin Hirsch,[c] Piter S. Miedema,[c] Bernd von Issendorff,[f] J. Tobias Lau,[c, f] and Thomas Schlathölter*[b]

Abstract: Preservation of protein conformation upon transfer into the gas phase is key for structure determination of free single molecules, for example using X-ray free-electron lasers. In the gas phase, the helicity of melittin decreases strongly as the protein's protonation state increases. We demonstrate the sensitivity of soft X-ray spectroscopy to the gas-phase structure of melittin cations ($[\text{melittin}+q\text{H}]^{q+}$, $q=2$–4) in a cryogenic linear radiofrequency ion trap. With increasing helicity, we observe a decrease of the dominating carbon 1s–π^* transition in the amide C=O bonds for non-dissociative single ionization and an increase for non-dissociative double ionization. As the underlying mechanism we identify inelastic electron scattering. Using an independent atom model, we show that the more compact nature of the helical protein conformation substantially increases the probability for off-site intramolecular ionization by inelastic Auger electron scattering.

In biological systems conformational changes in proteins take place in the liquid phase, which is where the established experimental techniques for protein folding studies are employed. Many of the most powerful approaches for molecular structure determination, however, are gas-phase techniques. Currently, the potential of these approaches to investigate protein structures is explored vigorously. A prime incentive is the experimental observation of protein dynamics with atomic resolution, a goal pursued by X-ray diffraction on nanocrystals or single proteins at X-ray free electron lasers.[1] Conservation of protein conformation upon transfer from solution to the gas phase is a key issue, and the field of native mass spectrometry is to a large extent based on this concept.[2,3]

In two pioneering experiments, it was recently shown that the combination of electrospray ionization (ESI) tandem mass spectrometry with synchrotron radiation in the soft X-ray regime can be used to study near edge X-ray absorption of gas-phase protonated proteins and peptides.[4,5] The method has then been employed to investigate protein conformation in the gas phase. For instance, whereas ubiquitin in its native (solution phase) protonation state keeps its compact conformation upon transfer into the gas phase,[6] much higher protonation induces unfolding due to Coulomb repulsion of the positively charged sites. This effect is manifest in X-ray spectra as a characteristic correlation of inner-shell ionization energy with protonation state.[7]

Here, we show the potential of inner-shell photoionization to reveal information on protein secondary structure. The secondary structure of melittin (2.8 kDa, 26 amino acid residues) in aqueous solution is dominated by α-helices. Helicity is preserved upon transfer into the gas phase for doubly protonated melittin while higher protonation strongly reduces gas-phase helicity.[8,9] For the native structure, see Figure 1.

We brought protonated melittin cations into the gas phase by means of electrospray ionization. Mass-selected $[\text{melittin}+q\text{H}]^{q+}$ ions ($q=2$–4) were then stored in a cryogenic ($T\approx 10$ K)

[a] Dr. S. Bari, Dr. R. Boll, Prof. Dr. S. Techert
DESY, Notkestr. 85, 22607 Hamburg (Germany)

[b] D. Egorov, Dr. T. L. C. Jansen, Prof. Dr. R. Hoekstra, Dr. T. Schlathölter
Zernike Institute for Advanced Materials, University of Groningen
Nijenborgh 4, 9747AG Groningen (The Netherlands)
E-mail: t.a.schlatholter@rug.nl

[c] Dr. V. Zamudio-Bayer, C. Bülow, Dr. R. Lindblad, G. Leistner, Dr. A. Ławicki, Dr. K. Hirsch, Dr. P. S. Miedema, Prof. Dr. J. T. Lau
Institut für Methoden und Instrumentierung der Forschung mit Synchrotronstrahlung, Helmholtz Zentrum Berlin für Materialien und Energie, Albert-Einstein-Str. 15, 12489 Berlin (Germany)

[d] C. Bülow, G. Leistner
Institut für Optik und Atomare Physik
Technische Universität Berlin, 10623 Berlin (Germany)

[e] Dr. R. Lindblad
Department of Physics, Lund University, 22100 Lund (Sweden)

[f] Dr. V. Zamudio-Bayer, Prof. Dr. B. von Issendorff, Prof. Dr. J. T. Lau
Physikalisches Institut, Universität Freiburg
Hermann-Herder-Straße 3, 79104 Freiburg (Germany)

[g] Prof. Dr. S. Techert
Institute of X-ray Physics
University of Göttingen, 37077 Göttingen (Germany)

Supporting information and the ORCID identification numbers for the authors of this article can be found under: https://doi.org/10.1002/chem.201801440.

linear radiofrequency ion trap,[10–12] a fixed endstation at the high-resolution and variable-polarization soft X-ray beamline UE52-PGM at the BESSY II synchrotron radiation facility. Due to low target density, photoabsorption cross-sections cannot be measured directly but require an action-spectroscopy approach. The photon energy is scanned stepwise over the carbon K edge (282–300 eV) and at each photon energy, the trap content is exposed to the monochromatic ($\Delta E = 250$ meV) soft X-rays and the photoproducts (intact proteins and fragments) are extracted into a time-of-flight mass spectrometer for mass analysis. Partial ion yields for non-dissociative single and double ionization of $[\text{melittin}+q\text{H}]^{q+}$ ($q = 2$–4) into $[\text{melittin}+q\text{H}]^{(q+n)+}$ ($n = 1,2$) are determined from the photoionization mass spectra. The combination of large trap volume and high resolution allows for the acquisition of photoionization spectra of excellent resolution and detail. Of particular relevance is the cryogenic temperature of the trapped ions. Here, the buffer gas cooling process involves a large number of collisions with He atoms and accordingly has a timescale up to the ms range. At the end of the cooling process, not only the transient conformations are frozen out. It is also very likely that the number of fundamental conformers is reduced in this process. This is different from for example supersonic jet cooling, where the freezing is very fast and typically the conformational space is much more conserved.

In the photoexcitation regime for photon energies below the carbon 1s ionization energy, photoabsorption induces the resonant transition of a 1s electron into an unoccupied valence orbital (for a sketch see left panel of Figure 1). For photon energies exceeding the 1s ionization energy, direct photoionization into the continuum is the dominating process (for a sketch, see left panel of Figure 2). We will first focus on the photoexcitation regime. The accessible unoccupied orbitals are energetically different, and are localized at different sites within the protonated protein. Photoexcitation leaves the system in a core-excited state that subsequently undergoes resonant Auger decay where the 1s vacancy is filled by a valence electron, accompanied by the simultaneous emission of an Auger electron from the same site. The charge state of a $[\text{melittin}+q\text{H}]^{q+}$ precursor increases by one. With much lower probability, two or more Auger electrons can be emitted.[13] For the carbon K-shell, single Auger electron emission is generally by far the dominant process.[14] Here we put forward a second mechanism leading to double ionization, which we will

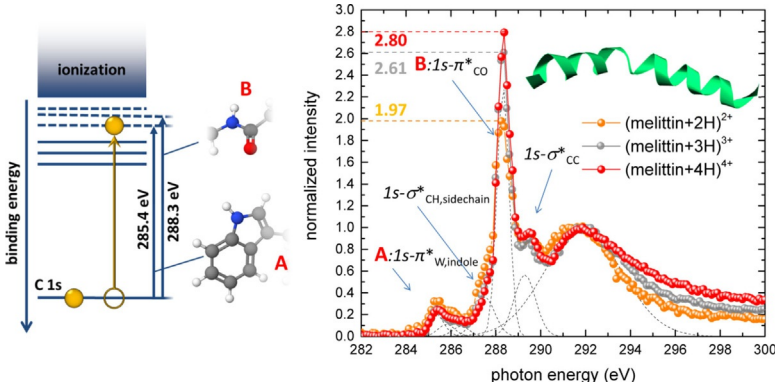

Figure 1. Left: Schematic for carbon 1s–π* photoexcitation (solid horizontal lines: occupied states; dashed horizontal lines: unoccupied states). The process is predominantly followed by a single Auger emission process, leaving the system singly ionized. Right: The partial ion yield for non-dissociative (melittin $+ q\text{H})^{q+}$ single ionization (NDSI) into $(\text{melittin}+q\text{H})^{(q+1)+}$ as a function of photon energy. All three spectra are normalized to the maximum of the broad feature near 291.5 eV. Ribbon diagram: native melittin solution structure.

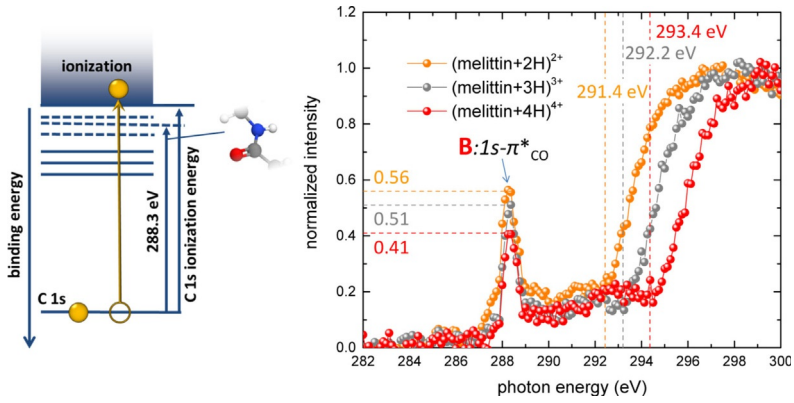

Figure 2. Left: Schematic for direct carbon 1s photoionization. Ionization is predominantly followed by a single Auger emission process, which implies an increase of the charge state by two. Right: The partial ion yield for non-dissociative $(\text{melittin}+q\text{H})^{q+}$ double ionization into $(\text{melittin}+q\text{H})^{(q+2)+}$ as a function of photon energy. The 1s ionization energies for the three protonation states are indicated. All spectra are normalized to the maximum of the double ionization continuum.

refer to as intramolecular ionization by off-site inelastic electron scattering (IES). In large molecules, such as proteins, emitted Auger electrons are likely to cause electron impact ionization at another site in the molecule, leading to emission of a secondary electron. Being non-local and depending on the probability of scattering at valence-electron density along the path of the primary Auger electron, the process can be sensitive to protein conformation, in contrast to the aforementioned double ionizations, which are of localized origin.

Depending on the protein size, soft X-ray photoionization can lead to small fragments (often immonium ions), sequence ions, as well as intact ionized proteins or ionized proteins that have lost neutral groups.[15] For melittin at room temperature, these channels are known to coexist.[16] At $T \approx 10$ K, in contrast, our data show that non-dissociative single and double ionization become the strongest channels.

Figure 1 displays the experimental data for non-dissociative single ionization (NDSI) of $[\text{melittin} + q\text{H}]^{q+}$ ($q = 2$–4). The dominant feature labeled **B** is centered at 288.34 eV with a FWHM of 0.63 eV for $q = 4$. This peak can be assigned to carbon 1s–π^* transitions in the C=O double bonds of the amide groups (see Figure 1) and is commonly observed for gas-phase amino acids at similar energy and peak-width.[17,18] For gas-phase and condensed-phase proteins at room temperature, slightly wider resonances have been observed.[4,5,7,19] The peak labeled **A** is composed of at least three different carbon 1s–π^* transitions, all involving carbon atoms from the bicyclic indole group of the tryptophan (W) sidechain. Two additional features at 287.5 and 289.7 eV are assigned to carbon 1s–σ^* transitions, for instance in the CH groups of aliphatic amino acid sidechains (287.5 eV) and in C–C bonds (289.7 eV). The latter peak has only been observed previously for gas-phase amino acids.[18] The unresolved broad structure centered at 291.9 eV is due to various transitions to σ^* and Rydberg orbitals. Note, that all three spectra are normalized to the maximum of the broad feature near 291.5 eV. Milosavljevic and co-workers normalized similar data for ubiquitin cations to the total peak area,[7] which makes sense for a large protein where fragmentation is weak. For melittin, fragmentation is a relevant channel which is different in magnitude for the different protonation states under study, and normalization to total peak area is not an option. An alternative normalization that we tried was on the intensity of resonance A. Unfortunately, the initial photoabsorption site can influence the balance between fragmentation and non-dissociative processes, in particular for aromatic sidechains [5] (such as W).

Before discussing Figure 1 in more detail, we first turn to the direct photoionization regime with photon energies above the 1s ionization threshold (for a sketch, see Figure 2, left panel). 1s Photoionization increases the charge state of $[\text{melittin} + q\text{H}]^{q+}$ from q to $q+1$. The resulting 1s core vacancy is subject to an Auger decay process with emission of a single Auger electron dominating, increasing the charge state further from $q+1$ *to* $q+2$.

The right panel of Figure 2 displays the experimental data for non-dissociative double ionization (NDDI) of $[\text{melittin} + q\text{H}]^{q+}$ ($q = 2$–4). The main feature in all three spectra is a sharp increase in intensity, once the photon energy overcomes the carbon 1s ionization energy. Below this threshold, there is evidence for the resonant carbon 1s–π^* excitation (labeled **B)** in the C=O bonds of the amide group. Peak **B** reflects Auger decays accompanied by emission of two electrons and/or by intramolecular ionization by off-site IES. All spectra are normalized to the maximum of the double ionization continuum.

Both sets of spectra in Figure 1 and Figure 2 show a clear protonation state dependence. First, we focus on photon energies exceeding ≈290 eV. For non-dissociative single ionization it is obvious that with increasing q the broad structure at high photon energies develops a tail on the high energy side (see Figure 1). With increasing protonation q, the threshold for direct photoionization increases and higher lying σ-states become bound states. The respective increase in carbon 1s ionization energy with q is evident in the NDDI data shown in Figure 2. The carbon 1s ionization energy, determined from the spectra as the onset of the ionization edge (indicated with a dashed line and labeled with the respective energy value) increases from 291.4 eV for $[\text{melittin} + 2\text{H}]^{2+}$ over 292.2 eV to 293.4 eV for $[\text{melittin} + 4\text{H}]^{4+}$.

For the much larger protein ubiquitin, Milosavljevic et al.[7] also observed an increase of carbon 1s ionization energy with protonation state, except for a small range of protonation states associated with conformational change, where ionization energies remained constant. Similar results had been observed by the same group previously, for VUV photoabsorption.[20] The authors rationalized their observations by a reduction in Coulomb repulsion of the protonated sites upon structural relaxation. The experimental finding is structurally unspecific in the sense that, for low protonation, ubiquitin has a complex conformation with a secondary structure including α-helices and β-sheets, and a superimposed tertiary structure and the authors boil the effect down to a dependence of the ionization energy on the inverse effective radius of the molecule. In contrast, the conformation of gas-phase $[\text{melittin} + 2\text{H}]^{2+}$ is dominated by α-helices, and helicity is already partly reduced in $[\text{melittin} + 3\text{H}]^{3+}$. From the observed increase in carbon 1s ionization energies (see Figure 2), it is however clear that melittin's structural relaxation with increasing q, that is, the loss of α-helicity, does not compensate for the increase in charge state.

A second and very important finding for NDSI is an increase of the relative strength of the carbon–carbon 1s–π^*_{CO} resonance (peak B) with protonation state with respect to all other spectral features, from 1.97 ± 0.05 ($q = 2$) over 2.61 ± 0.05 ($q = 3$) to 2.8 ± 0.05 ($q = 4$). Interestingly, in Figure 2 the opposite trend is observed for NDDI: Here, the relative intensity of the carbon 1s–π^*_{CO} resonance decreases as a function of protonation state, from 0.56 ± 0.05 ($q = 2$) via 0.51 ± 0.05 ($q = 3$) to 0.41 ± 0.05 ($q = 4$).

To understand the origin of this opposite trend, it is important to recall the different stages of the underlying sequence of atomic process and how these would be influenced by initial conformation:

i) Resonant 1s–π^* photoexcitation,

ii) Auger-decay, leading to the emission of one or more energetic Auger electron,
iii) Escape of the Auger electron from the protein.

For i) the dependence on the initial 1s–π* photoexcitation on protein secondary structure could explain the relative decrease of the carbon 1s–π^*_{CO} resonance in the NDSI spectra (Figure 1) but hardly the simultaneous increase of the same resonance in the NDDI spectra Figure 2). α-helical structure in proteins is stabilized by hydrogen bonds between an amide C=O group and an amide N–H group, four residues later in the sequence. The loss of helical structure implies loss of the hydrogen bonds and thus an altered electronic structure of molecular orbitals in the groups involved. Such an effect potentially influences oscillator strengths.

To quantify the effect of hydrogen bonding on carbon 1s–π* transition probabilities for an α-helical structure, we performed time-dependent density functional theory calculations on a model peptide. The details of the calculations are given in Supplementary materials. Briefly, a peptide consisting of 8 glycine residues was optimized for a straight structure, an α-helical structure and a β-hairpin. It is expected that gas-phase $[\text{melittin} + 2\,H]^{2+}$ contains even longer helical sections, comparable to the solution structure.[8] The oscillator strengths f_{OS} for the carbon 1s–π* transitions in the different carbonyl groups were then calculated. The absolute energies exhibit the commonly observed offset, but it is clear that for α-helix and β-hairpin, transition energies are systematically lower (up to ≈0.3 eV) as compared to the linear chain reference. This follows the trend observed experimentally, where a small shift (≈0.15 eV) is observed. The transition probabilities for all residues are smaller for the helix (with a minimum $f_{OS} = 0.0479$ for residue 6) than for the linear chain ($f_{OS} = 0.0607$ for residue 6). The average decrease is 13% for the helix and still 4% for the β-sheet. The experiment however averages over an entire ensemble of low-energy melittin conformations many of which are only partly helical,[8] that is, the 13% reduction is an upper limit. Most importantly, the reduction of the resonance would be expected not only for NDSI but also for NDDI, for which exactly the opposite trend is observed.

Concerning (ii), the Auger decay process filling the 1s vacancy could in principle be influenced by the same weak dependence of the electronic structure on helicity, as discussed in (i). However, each single Auger decay event involves two valence orbitals. Experimentally, a superposition of all possible combinations is contributing to a spectrum, that is, possible weak electronic structure effects are likely to be washed out.

Finally (iii), the escape of an emitted Auger electron from the protonated protein is expected to be very sensitive to the protein conformation, because the probability for off-site IES increases with the number of atoms passed on the electrons way out. In valence photoionization experiments on neutral noble gas clusters, inelastic photoelectron scattering has been observed earlier and its contribution was found to increase with cluster size.[21] However, the effect has never been used to investigate spatial conformations of molecular systems. As obvious from the top panels in Figure 3, for melittin in both

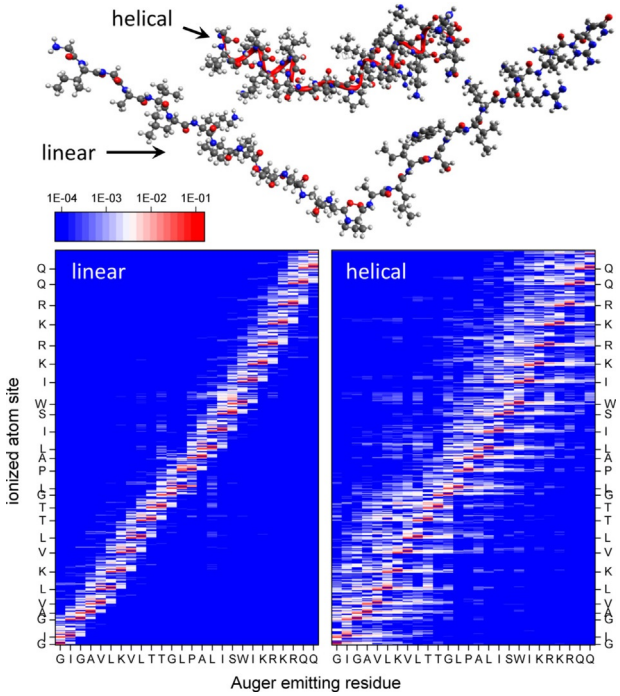

Figure 3. Probabilities for ionization by off-site IES at the carbon 1s–π^*_{CO} resonance, obtained from a Monte Carlo simulation. Top panels: melittin linear[27] and helical[28] model geometries. Bottom panels: Simulation results as 2D arrays; *x*-axis: Auger-emitting residue (one-letter code); *y*-axis: numeric position of the ionized atom (start of a new residue indicated by one-letter code). Probabilities between 10^{-4} and 10^{-1} are given in color code on a logarithmic scale.

linear and helical conformation, the amino acid residues are sticking out from the backbone, meaning that electrons emitted from the residues will be less influenced by the helical structure, whereas electrons emitted from the backbone will experience dramatic changes along their path.

For quantification we developed a Monte Carlo model that is conceptually based on the independent atom model (IAM), often employed in electron scattering from molecular systems.[22,23] The IAM is based on the fact that for sufficiently high electron kinetic energies, elastic and inelastic electron scattering cross-sections can be approximated using the single-atom cross-sections of the molecular constituents. The Auger electron spectrum for gas-phase glycine has been measured very recently and is dominated by a broad, structured band between 225 and 260 eV that is centered at about 250 eV[24] and we assume this to be a good approximation for carbon 1s Auger electrons from a protein as well. For electron energies exceeding 200 eV, deviations of IAM inelastic scattering cross-sections from experimental data for molecules such as CO_2 are typically smaller than 10%.[22] A similar accuracy can be expected for a large molecule such as melittin. We have therefore used the data for electron impact cross-sections for the H, C, N and O constituents at 250 eV.[25,26] For each melittin residue, 10^5 electrons are launched into random directions, starting from the respective carboxyl carbon atom in the residues' amide group. For each trajectory it is determined whether it leads to electron impact ionization of another melittin

constituent. The result for each initial carboxyl carbon site is an electron impact ionization probability for each atom in the system. We have computed these data for two different melittin geometries. A linear conformation was computed using the Avogadro package.[27] As a typical helical conformation, we chose the melittin entry in the protein database.[28] In both cases, ionization probabilities maximize to about 7% for the neighboring O atom and for the C_α atom and quickly decrease with increasing distance from the Auger-emitting carbon atom. The results are shown in Figure 3.

For the linear conformation, isotropic emission from any site leaves most Auger electrons unobstructed, once they have passed the directly neighboring atoms. Emission along the chain is statistically irrelevant and a narrow distribution of ionized atoms is observed, typically involving mostly atoms from the emitter residue and its direct neighbors. The average total probability for ionization by off-site IES is $P_{\text{ionization}}(\text{linear}) = 0.33$.

For the helix case, the molecule is far more compact. Here, Auger electrons are very likely to interact with atoms from residues further up or down the sequence, in addition to atoms from the emitter residue and direct neighbors. A much wider distribution of ionized sites is observed. The average total probability for ionization by off-site IES is $P_{\text{ionization}}(\text{helix}) = 0.45$.

According to these calculations, emission of a single Auger electron upon resonant carbon 1s–π^*_{CO} excitation has a conformation dependent probability for ionization via off-site IES, leading to removal of a second electron. For NDSI we are interested in the fraction of Auger emission events that do not lead to further ionization. $(1-P_{\text{ionization}}(\text{linear}))/(1-P_{\text{ionization}}(\text{helix})) = 1.22$ is the relevant quantity which compares qualitatively well with the decrease of the carbon 1s–π^*_{CO} resonance Figure 1 (2.8/1.97 = 1.42). The experimentally determined ratio depends on the normalization, which makes a precise quantitative comparison difficult. For NDDI, the ionization events are relevant. $P_{\text{ionization}}(\text{linear})/P_{\text{ionization}}(\text{helix}) = 0.73$ is the relevant quantity, which needs to be compared to the increase of the carbon 1s–π^*_{CO} resonance in Figure 2 (0.41/0.56 = 0.73). For NDDI, the normalization is more straightforward and the agreement between simulation and experiment is better.

Near edge X-ray absorption spectroscopy is clearly sensitive to the melittin secondary structure via off-site inelastic electron scattering. The mechanism is similar to H/D exchange experiments, where the fraction of H sites that is exposed to the outside is determined—helix formation then lowers the signal.[9] Inelastic mean free paths of 1.2–1.5 nm have been determined theoretically for 300–500 eV electrons in a model protein.[29] This path length is comparable to the diameter of an α-helix (1.2 nm), which is the characteristic length in our experiment. In future studies, we will therefore systematically investigate off-site IES in larger proteins with compact tertiary structures. For these, off-site IES will likely induce multiple ionization when originating from Auger-emitting residues deep within the protein.

Acknowledgements

We thank HZB for the allocation of synchrotron radiation beamtime at beamline UE52-PGM. The research leading to these results has received funding from the European Community's Seventh Framework Programme (FP7/2007–2013) under grant agreement no. 312284. B.v.I. acknowledges financial support from the BMBF-Projekt 05K16VF1. S.B. was supported by the Helmholtz Initiative and Networking Fund through the Young Investigator Groups Program. S.B. and S.T. acknowledge support from the Deutsche Forschungsgemeinschaft, project B03/SFB755. R.L. acknowledges the Swedish Research Council (637-2014-6929).

Conflict of interest

The authors declare no conflict of interest.

Keywords: Auger electrons · gas-phase biomolecules · mass spectrometry · protein conformation · soft X-ray spectroscopy

[1] S. Boutet, L. Lomb, G. J. Williams, T. R. M. Barends, A. Aquila, R. B. Doak, U. Weierstall, D. P. DePonte, J. Steinbrener, R. L. Shoeman, M. Messerschmidt, A. Barty, T. A. White, S. Kassemeyer, R. A. Kirian, M. M. Seibert, P. A. Montanez, C. Kenney, R. Herbst, P. Hart, J. Pines, G. Haller, S. M. Gruner, H. T. Philipp, M. W. Tate, M. Hromalik, L. J. Koerner, N. van Bakel, J. Morse, W. Ghonsalves, D. Arnlund, M. J. Bogan, C. Caleman, R. Fromme, C. Y. Hampton, M. S. Hunter, L. C. Johansson, G. Katona, C. Kupitz, M. Liang, A. V. Martin, K. Nass, L. Redecke, F. Stellato, N. Timneanu, D. Wang, N. A. Zatsepin, D. Schafer, J. Defever, R. Neutze, P. Fromme, J. C. H. Spence, H. N. Chapman, I. Schlichting, *Science* **2012**, *337*, 362–364.

[2] A. J. R. Heck, *Nat. Methods* **2008**, *5*, 927–933.

[3] C. Uetrecht, I. M. Barbu, G. K. Shoemaker, E. van Duijn, A. J. R. Heck, *Nat. Chem.* **2011**, *3*, 126–132.

[4] A. R. Milosavljević, F. Canon, C. Nicolas, C. M. L. Nahon, A. A. Giuliani, *J. Phys. Chem. Lett.* **2012**, *3*, 1191–1196.

[5] O. González-Magaña, G. Reitsma, M. Tiemens, L. Boschman, R. Hoekstra, T. Schlathölter, *J. Phys. Chem. A* **2012**, *116*, 10745.

[6] T. Wyttenbach, M. T. Bowers, *J. Phys. Chem. B* **2011**, *115*, 12266–12275.

[7] A. R. Milosavljević, C. Nicolas, M. L. J. Rankovic, F. Canon, C. Miron, A. Giuliani, *J. Phys. Chem. Lett.* **2015**, *6*, 3132–3138.

[8] H. V. Florance, A. P. Stopford, J. M. Kalapothakis, B. J. McCullough, A. Bretherick, P. E. Barran, *Analyst* **2011**, *136*, 3446.

[9] S. E. Evans, N. Lueck, E. M. Marzluff, *Int. J. Mass Spectrom.* **2003**, *222*, 175–187.

[10] K. Hirsch, J. T. Lau, P. Klar, A. Langenberg, J. Probst, J. Rittmann, M. Vogel, V. Zamudio-Bayer, T. Möller, B. von Issendorff, *J. Phys. B* **2009**, *42*, 154029.

[11] A. Langenberg, K. Hirsch, A. Lawicki, V. Zamudio-Bayer, M. Niemeyer, P. Chmiela, B. Langbehn, A. Terasaki, B. V. Issendorff, J. T. Lau, *Phys. Rev. B* **2014**, *90*, 184420.

[12] M. Niemeyer, K. Hirsch, V. Zamudio-Bayer, A. Langenberg, M. Vogel, M. Kossick, C. Ebrecht, K. Egashira, A. Terasaki, T. Möller, B. v. Issendorff, J. T. Lau, *Phys. Rev. Lett.* **2012**, *108*, 057201.

[13] L. Journel, R. Guillemin, A. Haouas, P. Lablanquie, F. Penent, J. Palaudoux, L. Andric, M. Simon, D. Ceolin, T. Kaneyasu, J. Viefhaus, M. Braune, W. B. Li, C. Elkharrat, F. Catoire, J.-C. Houver, D. Dowek, *Phys. Rev. A* **2008**, *77*, 042710.

[14] M. Krause, *J. Phys. Chem. Ref. Data* **1979**, *8*, 307–327.

[15] L. Schwob, M. Lalande, D. Egorov, J. Rangama, R. Hoekstra, V. Vizcaino, T. Schlatholter, J. Poully, *Phys. Chem. Chem. Phys.* **2017**, *19*, 22895–22904.

[16] D. Egorov, L. Schwob, M. Lalande, R. Hoekstra, T. Schlatholter, *Phys. Chem. Chem. Phys.* **2016**, *18*, 26213 – 26223.
[17] V. Feyer, O. Plekan, R. Richter, M. Coreno, K. C. Prince, V. Carravetta, *J. Phys. Chem. A* **2008**, *112*, 7806 – 7815.
[18] O. Plekan, V. Feyer, R. Richter, M. Coreno, M. de Simone, K. C. Prince, V. Carravetta, *J. Electron Spectrosc. Relat. Phenom.* **2007**, *155*, 47 – 53.
[19] Y. Zubavichus, A. Shaporenko, M. Grunze, M. Zharnikov, *J. Phys. Chem. B* **2008**, *112*, 4478 – 4480.
[20] A. Giuliani, A. R. Milosavljević, K. Hinsen, F. Canon, C. Nicolas, M. Refregiers, L. Nahon, *Angew. Chem. Int. Ed.* **2012**, *51*, 9552; *Angew. Chem.* **2012**, *124*, 9690.
[21] U. Hergenhahn, A. Kolmakov, M. Riedler, A. de Castro, O. Lofken, T. Moller, *Chem. Phys. Lett.* **2002**, *351*, 235 – 241.
[22] F. Blanco, G. Garcia, *Phys. Lett. A* **2004**, *330*, 230 – 237.
[23] F. Blanco, G. García, *Phys. Lett. A* **2003**, *317*, 458 – 462.
[24] A. Sanchez-Gonzalez, T. R. Barillot, R. J. Squibb, P. Kolorenc, M. Agaker, V. Averbukh, M. J. Bearpark, C. Bostedt, J. D. Bozek, S. Bruce, S. C. Montero, R. N. Coffee, B. Cooper, J. P. Cryan, M. Dong, J. H. D. Eland, L. Fang, H. Fukuzawa, M. Guehr, M. Ilchen, A. S. Johnsson, C. Liekhus-S, A. Marinelli, T. Maxwell, K. Motomura, M. Mucke, A. Natan, T. Osipov, C. Ostlin, M. Pernpointner, V. S. Petrovic, M. A. Robb, C. Sathe, E. R. Simpson, J. G. Underwood, M. Vacher, D. J. Walke, T. J. A. Wolf, V. Zhaunerchyk, J. Rubensson, N. Berrah, P. H. Bucksbaum, K. Ueda, R. Feifel, L. J. Frasinski, J. P. Marangos, *J. Phys. B* **2015**, *48*, 234004.
[25] E. Brook, M. Harrison, A. Smith, *J. Phys. B* **1978**, *11*, 3115 – 3132.
[26] Y.-K. Kim, J.-P. Desclaux, *Phys. Rev. A* **2002**, *66*, 012708.
[27] M. D. Hanwell, D. E. Curtis, D. C. Lonie, T. Vandermeersch, E. Zurek, G. R. Hutchison, *J. Cheminf.* **2012**, *4*, 17.
[28] D. S. Perekalin, V. V. Novikov, A. A. Pavlov, I. A. Ivanov, N. Y. Anisimova, A. N. Kopylov, D. S. Volkov, I. F. Seregina, M. A. Bolshov, A. R. Kudinov, *Chem. Eur. J.* **2015**, *21*, 4923 – 4925.
[29] Z. Tan, Y. Xia, M. Zhao, X. Liu, *Radiat. Environ. Biophys.* **2006**, *45*, 135 – 143.

Manuscript received: March 21, 2018
Revised manuscript received: April 3, 2018
Accepted manuscript online: April 10, 2018
Version of record online: May 3, 2018

